IEEE Access
Multidisciplinary | Rapid Review | Open Access Journal

Received July 21, 2021, accepted September 19, 2021, date of publication September 29, 2021, date of current version November 2, 2021.

*Digital Object Identifier 10.1109/ACCESS.2021.3116113*

# Coverage Enhance in Boundary Deployed Camera Sensor Networks for Airport Surface Surveillance

**WEI LI, XIANGTONG WANG, AND SONGCHEN HAN**
School of Aeronautics and Astronautics, Sichuan University, Chengdu 610017, China

Corresponding author: Wei Li (li.wei@scu.edu.cn)

This work was supported in part by Sichuan Science and Technology Program under Grant 2020YFG0134, and in part by Sichuan University under Grant 2020SCUNG205.

**ABSTRACT** Unlike the conventional coverage issue in camera sensor networks, the airport surface surveillance brings new challenges for achieving the desirable coverage. One of the biggest challenges comes from the deployment of camera sensors, i.e. due to the consideration of safety, the cameras are always installed on the land-side facilities in airports. In this paper, we propose a coverage enhancing method by deploying additional cameras for the boundary deployed heterogeneous camera networks. We convert the area coverage problem to maximize the barrier coverage in the area of interest by a boundary deployed camera network. The proposed method is divided into three phases: detecting the uncovered gaps in barriers; finding the optimal positions for deploying additional cameras; and optimizing the orientation of the additional cameras to cover the uncovered gaps. The simulation results confirm that our algorithm has better performance in coverage improvement and additional camera usage compared with other related methods.

**INDEX TERMS** Airport surface surveillance, camera networks, boundary deployed cameras, coverage enhance.

## I. INTRODUCTION

Among the participants of the air transportation system, airports play a vital role for providing a safe and efficient transition of passengers and goods between the ground and the airspace, which must operate daily to ensure the takeoff and landing activities of aircrafts in a safe and orderly manner. Since cameras can provide the fine-grained information about the airport surface, the applications of cameras in airport surveillance are becoming more and more extensive [1]–[3]. With the development of communication and computation technology, camera networks are capable of providing wide field of views and automatically capture any movement in the region of interest with 24-7 service [4], which leads them to be very adaptive in the surveillance for airport surface.

In camera networks, coverage is one of the important issues to be addressed, which indicated how well a region is monitored [5]. There are extensive studies concerning the coverage problem of sensor networks under different conditions and constraints from different perspectives. Usually, the coverage problem can be classified into three categories [6]: the area coverage, i.e. to cover a given a region of interest (ROI), the point coverage, i.e. to cover a set of special points, and the barrier coverage, i.e. to cover a barrier line in a ROI for detecting moving targets. In the airport surface surveillance, we not only focus on the special points in the airport or mobile objects crossing the airport, but also have to pay much attention to what is happening inside the airport surface. For example, it is dramatically important to provide full-view coverage of the whole airport surface for the controllers or operators to obtain the overall situation of airports. Therefore, in this study, we focus on the area coverage problem of the airport surface surveillance.

In most of conventional studies about the coverage problem, sensors are modeled as omnidirectional ones that have omniangle of sensing range, where the sensing region of a sensor is represented as a disk, shown as in Fig.1 (a) and the coverage only relies on the locations of sensors [7]. Unlike the omnidirectional sensors, a camera has the limited field of view (FOV). The coverage in camera networks is determined by not only the distribution of cameras, but also the sensing orientations of cameras. Therefore, coverage problem in camera network remains an open research topic. Besides, the particularities of airport surface surveillance bring new challenges for addressing the coverage problem. First of all, for the sake of safety, cameras always have to be installed

The associate editor coordinating the review of this manuscript and approving it for publication was Wenbing Zhao.

on the land-side facilities and buildings, such as terminal buildings, air traffic control towers, boarding bridges, etc. The cameras in airport surface belong to a kind of boundary deployment [8]. The coverage improvement approaches where the cameras can be located in any place among the ROI are not adaptive to the boundary deployed cameras. Besides, in airport surface, fixed perspective cameras are the most commonly utilized cameras which have the fixed positions, orientations, and focal lengths. This kind of cameras can provide fixed scene information about the airport and they are beneficial to cultivate the situational awareness for the operators or controllers. The methods that rotate the orientations of cameras to enhance the coverage cannot be used in the airport surface surveillance.

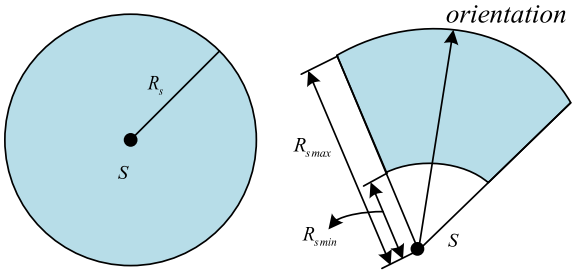


**FIGURE 1.** Sensing models of omnidirectional sensor and camera sensor.

In order to meet the above challenges, we adopt the sector band model to represent the perception range of the top-down sensing cameras rather than the simply sector model, shown as in Fig.1(b). Besides, for resolving the difficulty which comes from the different focus lengths of heterogeneous sensors, we map the area coverage problem for a ROI into a barrier coverage problem for a group of barrier lines. The interval between barriers is determined according to the focus lengths. We investigate the relationships between the barrier line and the sensing model of cameras. Based on the analysis, we propose a method for maximizing the coverage of the entire barrier group by deploying additional cameras as fewer as possible. The simulations verify that the proposed method has better performance than other related algorithms and achieve near-optimal results. The main contributions of this paper are as follows:

1) We analyze the effects of a camera's orientation on the coverage of a barrier line, and find the optimal orientation for maximizing the coverage.

2) We propose a method based on the geometric relationships between the barrier lines and sensing ranges of cameras to improve the coverage. We firstly detect uncovered gaps on barrier lines, and then find the optimal possible positions for deploying additional cameras according to relationships between the barrier and the sensing model. The orientations of the additional cameras are also optimized to cover the uncovered gaps in our proposed method.

The remainder of the paper is organized as follows: Section II summarizes the related work on area coverage as well as barrier coverage in camera networks. Section III describes the problem and the models that will be used in the paper. Section IV provides the coverage enhancing method in detail. In Section V, we conduct simulations to assess the performance of the proposed method. Finally, we conclude the paper in Section VI.

## II. RELATED WORK

Coverage problem is a fundamental issue in sensor networks about the quality of sensing. There are many excellent studies about the coverage problem in omniangle sensor networks. For instances, Wang *et al.* use Voronoi diagram to divide a ROI, and propose a method to determine the dynamic nodes with the limited movement for barrier covering the blind spot in the deployed area [9]. Li *et al.* propose a tree-based method to indicate the locations, sizes and shapes of coverage holes and then provide a healing method for improving the coverage [10]. Wang *et al.* propose a discrete approximation algorithm to achieve complete coverage based on a confident information coverage model in randomly deployed sensor networks [11].

Due to the differences between the omniangle sensors and the directional sensors, the study of coverage in directional sensor networks also has attracted much attention. He *et al.* propose a method to use the minimum number of cameras to provide the full area coverage in a 2-D continuous domain [12]. In their study, they have proven that minimum-number full-view coverage is a NP-hard problem and only suboptimal solution can be found. Eldrandaly *et al.* introduce an artificial intelligence algorithm to adjust the orientations of cameras for increasing the coverage of the PTZ surveillance system [13]. Sung *et al.* propose a distributed greedy algorithm based on Voronoi diagram to adjust the orientations of sensors to improve the effective field coverage of directional sensor networks [14]. Jia *et al.* formalize the maximizing full-view target coverage problem as a linear programming problem, and provide an optimal method to solve the problem in polynomial time [15]. Zhang *et al.* design a pitch angle optimization, a deflection angle optimization and a redundant node sleeping method to maximize the coverage in a directional 3D wireless sensor network [16]. Some scholars introduce coverage degree concept to measure the detection probability of targets in a ROI [17]. They construct the coverage coverage-degree problem as a constraint optimization problem and use a harmony search based approach to enhance the coverage. Han *et al.* provide a camera planning approach to optimize camera coverage for area surveillance [18]. In their approach, the coverage of cameras is inferred by using building footprints, points of interests, and WeChat data. They also maximize the coverage of cameras by considering the partial coverage of the demand unit area by using multi-source location-based service data. Yildiz *et al.* provide a bi-level optimal method to find optimal camera placement for providing angular coverage in wireless video sensor networks [19]. Although they consider the homogeneous and heterogeneous camera

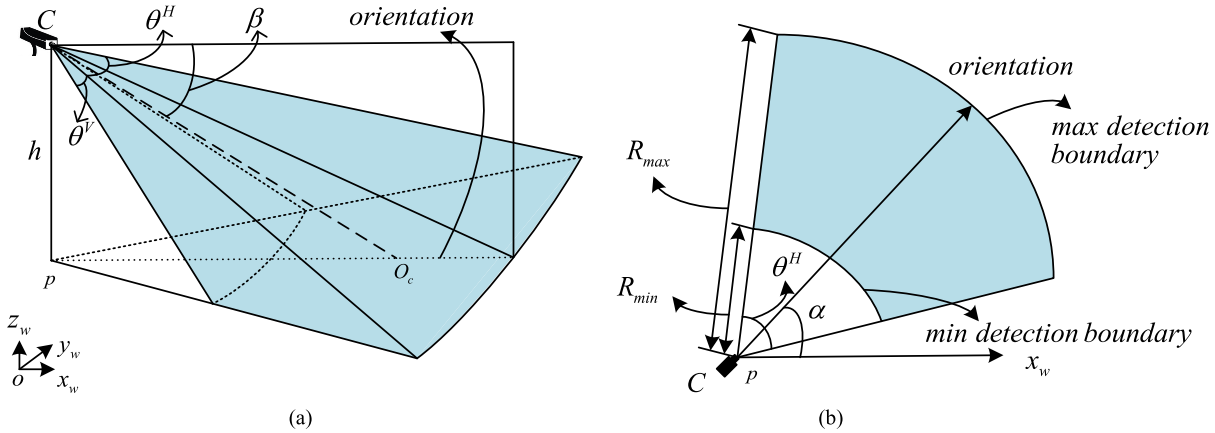


**FIGURE 2.** Sensing model of cameras.

deployment problem, the coverage scheme is provided only for satisfying the resolution requirements for certain areas of the ROI.

Barrier coverage is another important research issue in camera sensor networks. Due to the random deployment of sensors or damage of sensors in long-term working, barrier gaps may exist. Many studies proposed different approaches to discover the barrier gaps and then mend them. Xu *et al.* propose a decentralized mechanism to construct a disjoint full-view barrier by using visual sensors as few as possible [20]. In their method, the region is partitioned into a number of grids, which can reduce the computation cost and communication cost. Cheng and Wang use mobile sensors to avoid the barrier breach problem in a wireless sensor network [21]. Their method does not need to remove crossing barriers and has advantages in flexible arrangement of the sleep-wakeup schedule. For the barrier coverage in camera networks, another challenge comes from the directional sensing characteristic of camera sensors. In order to improve the barrier coverage, it is necessary to consider not only the deployment of sensors but also the sensing directions. Chen *et al.* study how to find barrier gaps and mend them by rotating the sensing directions of sensors in a lined-based deployed directional sensor network [22]. In their study, the weak and the strong barrier coverage are addressed by simple rotation algorithm and chain-reaction rotation algorithm, respectively. Cheng *et al.* take the image quality into consideration in the barrier gap coverage problem of visual sensor networks [23]. They propose a camera sensor selection method to form the barrier with consideration of importance of images. They also claim that the number of camera for barrier construction when cameras have rotation capability can be reduced. Khanjary *et al.* utilize distributed learning automata to find a near-optimal number of strong barrier lines in adjustable-orientation directional sensor networks [24]. They introduce a directional barrier graph to be used as a basis for improving the coverage of camera networks. Wu and Cardei propose a distributed method for the line-based sensor deployment to achieve weak and strong barrier coverage in wireless sensor networks consisting of directional sensors [25]. Their main idea is to rotate the orientations of sensors to minimize the number of coverage gaps.

The review of the existing studies on coverage issue of camera networks indicates that little effort has been made for the boundary deployed camera networks. In our study, three major issues are addressed: (1) we use sector band model to define the coverage range of cameras; (2) we consider the constraints in boundary deployed cameras; and (3) we provide an optimization method to determine the possible locations and orientations for deploying additional cameras according to relationships between the barrier and the sensing model.

## III. MODEL AND PROBLEM DESCRIPTION

### A. REGION OF INTEREST

Suppose that a camera network is randomly deployed along boundaries of a ROI for monitoring the activities cooperatively. Specifically, we assume that the ROI is a rectangle field with the length $l$ and the width $w$. The camera network containing $C$ cameras is located at one boundary of the rectangle. We also assume that cameras are fixed at the boundary once they are initially mounted.

In order to obtain information and detect events of every part in the ROI, it is necessary to rely on multiple cameras with different focus lengths. The cameras with the short focus lengths are usually used to monitor the near regions, because they have relative wide FOVs and short depth of views (DOVs) and can collect as much information as possible. The cameras with the long focus lengths are responsible for monitoring the regions that are far away from the cameras, because they have large DOVs and could provide the magnified images but with narrow FOVs. Therefore, in the airport surface surveillance, a number of heterogeneous cameras are used to cover a rectangle ROI.

### B. CAMERA SENSING MODEL

The cameras in airport are usually placed at the high positions for enlarging the FOVs and avoiding occlusions, which leads

to the top-down sensing orientation. In this study, the sensing model of a camera can be described as follows. The camera is located at the position $(x, y)$ in $x_w o y_w$ plane with the height $h$. The FOVs in horizontal and vertical directions are $\theta^H$ and $\theta^V$, respectively. $\alpha$ is the angle of camera's orientation relative to the $x_w$-axis. When the angle is along with the $x_w$-axis, $\alpha = 0$, and rotating in counter-clockwise is positive. $\beta$ is the tilt angle of the camera which is defined as the angle between the visual axis of the camera $CO_c$ and the $x_w o y_w$ plane. The traditional sensing model of cameras is always described as a sector region. However, due to existence of the height $h$ and the tilt angle $\beta$, the sensing space is actually an irregular rectangle pyramid, show as the blue region in Fig.2 (a).

Since the coverage of airport surface belongs to the problem of area coverage, we use a 2D model to represent the actual sensing space of the camera. Different from the conventional camera sensing models where the sector area is used, we adopt the sector band model to represent the sensing area of the camera, which is generated from the intersection between the sensing rectangle pyramid and the airport surface plane, shown as the blue area in Fig.2 (b). As shown in Fig.2 (b), the camera $C$ is located at the position $p$ with the coordinate $(x, y)$. Due to that the different cameras have different focus lengths, different tilt angles, and different placement heights, their corresponding 2D sensing areas are distinct. Although the sensing range can be enlarged by adjusting the tilt angles of cameras, the fixed perspective cameras always have their optimal sensing ranges with maximal object detection probabilities. Thus, for each fixed perspective camera, we can use $(p, \alpha, \theta^H, R_{\min}, R_{\max})$ to describe the sensing model. $R_{\min}$ and $R_{\max}$ denote the minimum and maximum detection range, respectively.

With such model, a point $s$ with the coordinate $(x_s, y_s)$ is considered to be covered by a camera, if the following conditions are satisfied.

1) The distance between the point and the camera is within the range $[R_{min}, R_{max}]$.

$$R_{\min} \leq |p - s| \leq R_{\max} \tag{1}$$

where $|\cdot|$ denotes the Euclidean distance.

2) The angle between the vector from $p$ to $s$ and the orientation of the camera is located within the horizontal FOV of the camera.

$$\alpha - \frac{\theta^H}{2} \leq \arctan\left(\frac{y_s - y}{x_s - x}\right) \leq \alpha + \frac{\theta^H}{2} \tag{2}$$

### C. PROBLEM DESCRIPTION

For a full area coverage problem, traditionally, it is necessary to make sure that every point in a ROI is detected or monitored by at least one camera. However, in practice, it is very difficult to realize the full area coverage, because it requires a large number of cameras and has to deploy cameras exquisitely on the rigorous positions. Uncovered regions may unavoidably exist in a ROI due to many reasons, such as insufficient nodes, occlusions, unsatisfied deployment, and so on [10]. Especially for the boundary deployed camera network, due to the limitations of the installment locations, it is nearly impossible to full cover all the points in the ROI. Therefore, in this paper, we want to maximize the coverage of a ROI with a boundary deployed camera network as much as possible.

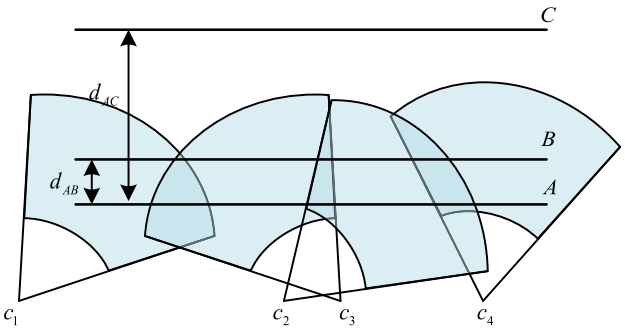


**FIGURE 3.** An example of barrier lines covered by cameras.

Actually, the problem of area coverage can be mapped into the problem of barrier coverage. It is easily proven that when a ROI is divided into a group of parallel straight barrier lines, if each barrier is fully covered by a camera network, every point in ROI will be also covered by the camera network.

From the strict mathematical perspective, since a line has no area theoretically, an area is composed of countless parallel lines, which makes the coverage of each line infeasible in practice. However, actually, it is unnecessary to require each line to be covered due to that the sensing model of cameras has a certain area. If a barrier is in the sensing range of a camera, its neighbor barriers are more likely to be also covered by the camera. We use an example to illustrate this point. As shown in Fig.3, the barrier line $A$ is covered by a camera network. The events on the barrier line $B$ which is close to $A$ are also collected by the camera network. In contrast, the barrier line $C$ that is far away from $A$ is out of the sensing range of the cameras. Therefore, we can use a group of barrier lines with an appropriate distance interval neither too big nor too small to approximately represent the ROI that needs to be covered. The big intervals will incur many coverage holes, and the small intervals bring many unnecessary cameras.

For the sake of simplification and computationally feasibility in practical applications, we select a group of barriers to approximately represent the ROI that need to be covered. The interval between barriers is $d_b$. We determine the value of $d_b$ based on the sensing ranges of camera. As mentioned before, in our study, the ROI coverage relies on heterogeneous cameras. Thus, the cameras with little sensing ranges determine the value of $d_b$, which is expressed as following.

$$d_b = R_{\max} - R_{\min} \tag{3}$$

Therefore, the area coverage problem is converted to maximize the barrier coverage for a group of parallel lines that makes up the area by a boundary deployed camera network. Since the camera network is composed of the fixed perspective cameras, once the cameras are deployed, the coverage

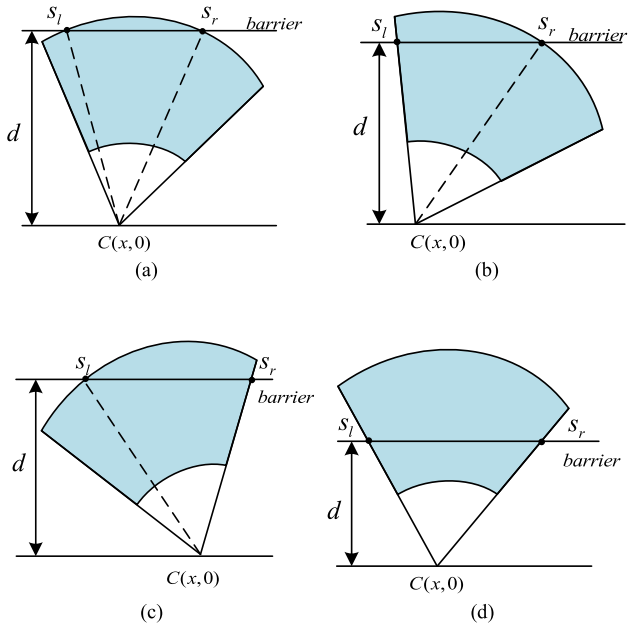


**FIGURE 4.** Relation between barrier and detection boundaries if $R_{min} < d < R_{max}$.

of the barriers is also determined. Thus, we have to deploy additional cameras to decrease the uncovered gaps of barriers. Therefore, in this paper, the coverage problem that needs to be addressed is to mend the uncovered gap by deploying additional cameras as few as possible.

## IV. COVERAGE ENHANCING METHOD

In this section, we propose a method for maximizing the coverage of the entire barrier group. Our proposed method is divided into three phases: 1) detect the uncovered gaps in barriers; 2) find the optimal positions for deploying additional cameras; and 3) optimize the orientation of the additional cameras to cover the uncovered gaps. In the following, we describe the three stages in detail.

### A. UNCOVERED GAP DETECTION

Since the positions of cameras and the locations of barriers are prior known, we can use the relationship between the distance and the two detection boundaries, $R_{max}$ and $R_{min}$, to estimate the coverage of the barrier line by a camera. We assume that the distance between the barrier line and the long boundary of ROI is $d$, and the camera is located at $(x, 0)$.

(1) If $\boldsymbol{d \geq R_{max}}$, there is no possibility that the camera covers any part of the barrier line.

(2) If $\boldsymbol{d > R_{min}}$ **and** $\boldsymbol{d < R_{max}}$, there will be four cases. In order to explain them clearly, we use the following expression to calculate the relation between $d$ and $R_{max}$:

$$\gamma = \arcsin \frac{d}{R_{\max}} \tag{4}$$

- The barrier will intersect the max detection boundary with two different point $s_l$ and $s_r$, and the line segment $s_l s_r$ on the barrier line will be covered by the camera, shown as the Fig.4 (a), when $\pi - 2\gamma \leq \theta^H$ and $(\gamma, \pi - \gamma) \in [\alpha - \theta^H/2, \alpha + \theta^H/2]$. The coordination of $s_l$ and $s_r$ in $x$ direction can be obtained by the following expression.

$$x_{s_l} = x - R_{\max}\cos\gamma, \quad x_{s_r} = x + R_{\max}\cos\gamma \tag{5}$$

- If $\pi - \gamma \notin [\alpha - \theta^H/2, \alpha + \theta^H/2]$, $\gamma \in [\alpha - \theta^H/2, \alpha + \theta^H/2]$, the two intersection points are on the max detection boundary and the left detection boundary, respectively. And, the line segment $s_l s_r$ on the barrier line will be covered by the camera, shown as the Fig.4 (b), where

$$x_{s_l} = x - \frac{d}{\tan(\alpha + \frac{\theta^H}{2})}, \quad x_{s_r} = x + R_{\max}\cos\gamma \tag{6}$$

- If $\pi - \gamma \in [\alpha - \theta^H/2, \alpha + \theta^H/2]$, $\gamma \notin [\alpha - \theta^H/2, \alpha + \theta^H/2]$, the barrier and the camera intersect at points $s_l$ and $s_r$. The line segment between $s_l$ and $s_r$ will be covered by the camera, as shown in Fig.4 (c):

$$x_{s_l} = x - R_{\max}\cos\gamma, \quad x_{s_r} = x + \frac{d}{\tan(\alpha - \frac{\theta^H}{2})} \tag{7}$$

- If $\gamma$ and $\pi - \gamma \notin [\alpha - \theta^H/2, \alpha + \theta^H/2]$, $\pi - 2\gamma > \theta^H$, and $\gamma < \alpha < \pi - \gamma$, the barrier will intersect the sensing region of the camera at the left and the right detection boundaries, respectively, shown as Fig.4 (d). We can obtain the covered line segment $s_l s_r$:

$$x_{s_l} = x - \frac{d}{\tan(\alpha + \frac{\theta^H}{2})}, \quad x_{s_r} = x + \frac{d}{\tan(\alpha - \frac{\theta^H}{2})} \tag{8}$$

(3) If $\boldsymbol{d \leq R_{min}}$, there are also five cases. In order to classify the five cases clearly, we calculate the relation between $d$ and $R_{min}$ by the expression:

$$\eta = \arcsin \frac{d}{R_{\min}} \tag{9}$$

- If $(\gamma, \eta) \in [\alpha - \theta^H/2, \alpha + \theta^H/2]$, the two intersection points are on the min and the max detection boundaries, respectively. The line segment $s_l s_r$ on the barrier line will be covered by the camera, shown as the Fig.5 (a). The coordination of $s_l$ and $s_r$ in $x$ direction can be obtained:

$$s_l = x + R_{\min}\cos\eta, \quad s_r = x + R_{\max}\cos\gamma \tag{10}$$

- If $\pi - \gamma$ and $\pi - \eta \in [\alpha - \theta^H/2, \alpha + \theta^H/2]$, as shown in the Fig.5 (b), the covered line segment $s_l s_r$ can be obtained by the expression:

$$x_{s_l} = x - R_{\max}\cos\gamma, \quad x_{s_r} = x - R_{\min}\cos\eta \tag{11}$$

- As shown in the Fig.5 (c), if $\eta \in [\alpha - \theta^H/2, \alpha + \theta^H/2]$, $\gamma \notin [\alpha - \theta^H/2, \alpha + \theta^H/2]$, and $\pi - 2\eta > \theta^H$, the covered line segment $s_l s_r$ becomes:

$$x_{s_l} = x + R_{\min}\cos\eta, x_{s_r} = x + \frac{d}{\tan(\alpha - \frac{\theta^H}{2})} \tag{12}$$

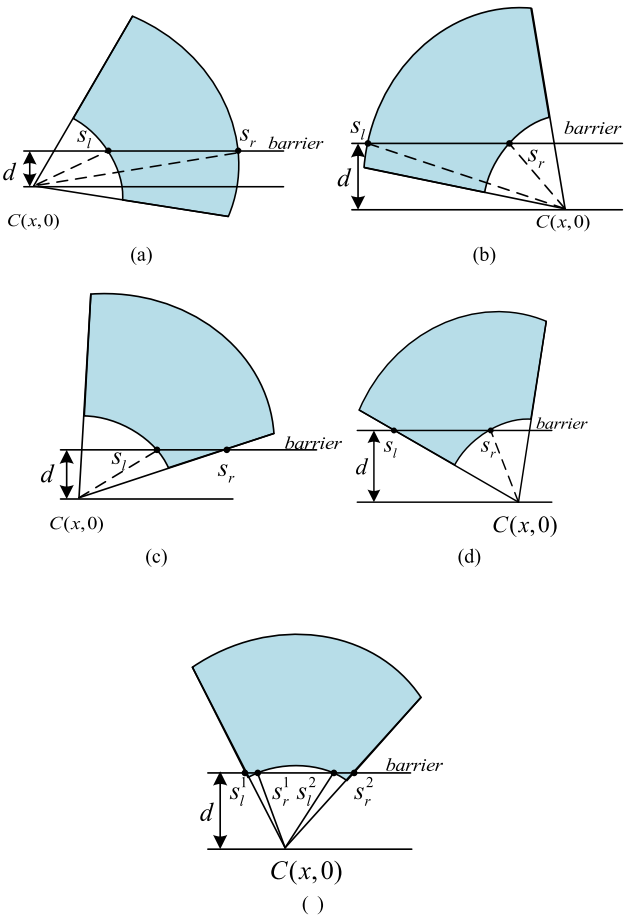


**FIGURE 5.** Relation between barrier and detection boundaries of cameras when $d < R_{\min}$.

- As shown in the Fig.5 (d), if $\pi - \eta \in [\alpha - \theta^H/2, \alpha + \theta^H/2]$, $\pi - \gamma \notin [\alpha - \theta^H/2, \alpha + \theta^H/2]$, and $\pi - 2\eta > \theta^H$, we can obtain the $s_l s_r$ by the following expression:

$$x_{s_l} = x - \frac{d}{\tan(\alpha + \frac{\theta^H}{2})}, \quad x_{s_r} = x - R_{\min}\cos\eta \tag{13}$$

- If $\pi - 2\eta > \theta^H$, $(\pi - \eta, \eta) \in [\alpha - \theta^H/2, \alpha + \theta^H/2]$, as shown in the Fig.5 (e), the covered line segments in the barrier line become two separated parts $s_l^1 s_r^1$ and $s_l^2 s_r^2$.

$$x_{s_l^1} = x - \frac{d}{\tan(\alpha + \frac{\theta^H}{2})}, \quad x_{s_r^1} = x - R_{\min}\cos\eta$$
$$x_{s_l^2} = x + R_{\min}\cos\eta, \quad x_{s_r^2} = x + \frac{d}{\tan(\alpha - \frac{\theta^H}{2})} \tag{14}$$

Therefore, by utilizing the above expressions, we can estimate the covered part of the barrier line by the $i^{th}$ camera, which is denoted as $(s_l s_r)_i$.The coverage of the barrier $Cov$ is the union of the covered barrier parts by the camera network $C$.

$$Cov = \bigcup_{i \in C} (s_l s_r)_i \tag{15}$$

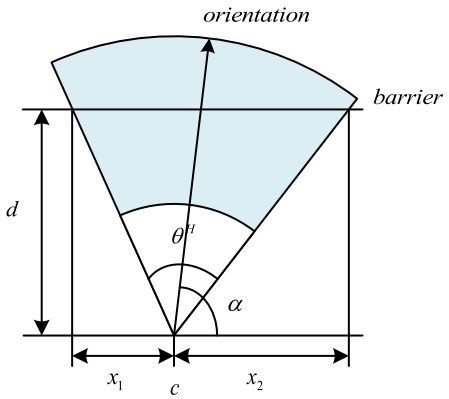


**FIGURE 6.** An example when $\alpha_{\min} < \alpha < \alpha_{\max}$.

For the $k^{th}$ barrier line $S_l^k S_r^k$, its coverage by the camera network $C$ is shown as:

$$Cov^k = \bigcup_{i \in C} (s_l s_r)_i^k \tag{16}$$

Thus, the uncovered gaps on the barrier are:

$$unCov^k = S_l^k S_r^k - \bigcup_{i \in C} (s_l s_r)_i^k \tag{17}$$

### B. FIND OPTIMAL LOCATIONS OF EXTRA SENSORS

Before presenting our algorithm for finding the optimal positions of additional cameras, we first prove a lemma that will be used in the algorithm.

*Lemma 1:* Consider that the distance between a camera and a barrier line is $d$. The FOV of the camera is $\theta$. If and only if the orientation of the camera is toward $\arcsin d/R_{\max} + \theta/2$ or $\pi - \arcsin d/R_{\max} - \theta/2$, the covered segment of the barrier achieve maximum by the camera.

*Proof:* We use $\alpha_{\min}$ and $\alpha_{\max}$ to denote $(\arcsin d/R_{\max} + \theta/2)$ and $(\pi - \arcsin d/R_{\max} - \theta/2)$, respectively. Let $\alpha$ denote the orientation of the camera.

#### 1) $R_{min} < d < R_{max}$

Firstly, we analyze the case when $R_{min} < d < R_{max}$. If $\alpha \in [\alpha_{\min}, \alpha_{\max}]$, as shown in Fig.6, the intersected line segment between the camera and the barrier is $x_1 + x_2$.

$$x_1 = d/\tan(\pi - \alpha - \theta/2), \quad x_2 = d/\tan(\alpha - \theta/2) \tag{18}$$

$$x_1 + x_2 = \frac{2d\sin\theta}{\cos\theta - \cos 2\alpha} \tag{19}$$

when $\cos\theta - \cos 2\alpha$ takes the minimum value, $x_1 + x_2$ achieves the maximum. Since $\alpha \in [\alpha_{\min}, \alpha_{\max}]$, when $\alpha = \alpha_{\min}$ or $\alpha = a_{\max}$, $\cos 2\alpha$ achieves the maximum. Therefore, $x_1 + x_2$ will also be the maximum value.

If $\alpha < \alpha_{\min}$ or $\alpha > \alpha_{\max}$, it is easily proven that the covered line segment is also shorter than that when $\alpha = \alpha_{\min}$ or $\alpha = a_{\max}$. Thus, the If and only if the orientation of the camera is toward $\alpha_{\min}$ or $\alpha_{\max}$, the covered segment of the barrier achieve maximum by the camera.

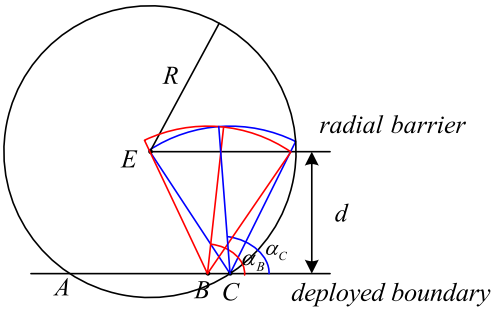


**FIGURE 7.** Coverage of a radial barrier by a camera.

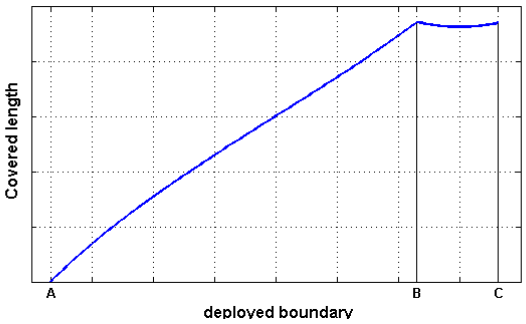


**FIGURE 8.** The lengths of covered barrier by the cameras.

2) $\boldsymbol{d < R_{min}}$

If $d < R_{min}$, there are three cases for the line segment covered by the camera. As shown in the Fig.5 (a) and Fig.5 (b), the length of the covered segment equals a constant value.

$$|s_l s_r| = R_{\max}\cos\gamma - R_{\min}\cos\eta \tag{20}$$

As shown in the Fig.5 (c) and Fig.5 (d), the covered length becomes:

$$|s_l s_r| = \frac{d}{\tan(\alpha - \frac{\theta}{2})} - R_{\min}\cos\eta \tag{21}$$

or

$$|s_l s_r| = \frac{d}{\tan(\alpha + \frac{\theta}{2})} - R_{\min}\cos\eta \tag{22}$$

When $\alpha = a_{\max}$ or $\alpha = a_{\min}$, $|s_l s_r|$ achieves maximum value $R_{\max}\cos\gamma - R_{\min}\cos\eta$.

When the camera covers the line as shown in Fig.5 (e), the covered length is:

$$|s_l s_r| = \frac{d}{\tan(\alpha - \frac{\theta}{2})} - \frac{d}{\tan(\alpha + \frac{\theta}{2})} - 2R_{\min}\cos\eta \tag{23}$$

Thus when $\alpha = \arcsin(d/R_{\min} + \theta/2)$ or $\alpha = \arcsin(d/R_{\min} - \theta/2)$, $|s_l s_r|$ achieves maximum $\frac{d}{\tan(\arcsin d/R_{\min}+\theta)} - R_{\min}\cos\eta$.

If $\alpha = a_{\max}$ or $\alpha = a_{\min}$, the covered line becomes :

$$|s_l s_r| = \frac{d}{\tan(\arcsin d/R_{\max} - \frac{\theta}{2})} - R_{\min}\cos\eta \tag{24}$$

Or

$$|s_l s_r| = \frac{d}{\tan(\arcsin d/R_{\max} + \frac{\theta}{2})} - R_{\min}\cos\eta \tag{25}$$

Due to that $\arcsin d/R_{\min} > \arcsin d/R_{\max}$, the covered barrier line achieves maximum, if and only if the orientation of the camera is towards $\alpha_{\min}$ or $\alpha_{\max}$. ■

Actually, the uncovered gaps on the barriers are always represented as line segments. The main difference between the line coverage and the segment coverage is how to deal with the end points of the segment. Thus, we have to analyze the scenarios of the end point coverage in different orientations of cameras.

*Corollary 1:* Consider a group of boundary deployed cameras with the same detecting range. For a radial barrier with the end point $E$, the subgroup of cameras that can cover $E$ is denoted as $C_E$. When $E$ is on the detection boundaries of cameras in $C_E$, the cameras whose orientation are towards $\arcsin(d/R_{\min} - \theta/2)$ or $\arcsin(d/R_{\min} - \theta/2)$ has the maximum coverage for the barrier.

*Proof:* The cameras that can cover $E$ are located within a circle with the radius $R$ and the center $E$, shown as in Fig.7. Specifically, for the boundary deployed cameras, the subgroup $C_E$ that covers $E$ is located on the line segment $AB$. When $E$ is on the detection boundaries of cameras in $C_E$, the covered part on the barrier achieve maximum if the orientations of cameras are towards $\arcsin(d/R_{\min} + \theta/2)$ or $\arcsin(d/R_{\min} - \theta/2)$ according to the ***Lemma* 1.** ■

Actually, according to ***Corollary*** 1, the optimal positions of cameras on the deployed boundary for covering the barrier line can be estimated. We use an example to illustrate the process. In order to cover the end point $E$ of the radial barrier, the cameras have to be located in the range between $A$ and $C$ on the deployed boundary. The lengths of covered barrier by the cameras on the boundary between $A$ and $C$ are shown as in Fig.8. The orientations of camera on $B$ and $C$ are $\alpha_B = \arcsin d/R_{\max} + \theta/2$ and $\alpha_C = \pi - \arcsin d/R_{\max} - \theta/2$, respectively, and the barrier coverage achieve maximal when cameras are located on B and C. Similarly, for a line segment barrier, we can also find the two other optimal positions of cameras whose sensing range covers another end point of the line segment. Therefore, there are four optimal potential positions for deploying an additional camera.

Note that optimal additional camera positions are related with sensing model of cameras. Generally, compared with the large sensing range cameras, the cameras with short sensing range have lower costs and requirements of installation. Therefore, for a certain uncovered gap, we chose the cameras with the smallest sensing range that can cover the end point of the gap.

### C. OPTIMIZING ORIENTATIONS OF CAMERAS

After we have found the optimal positions for deploying additional cameras, it is necessary to determine the orientations of these cameras. We also introduce a corollary to analyze the coverages in different orientations.

*Corollary 2:* Consider that the distance between a camera and a line segment with the end points $p_1$ and $p_2$ is $d$.

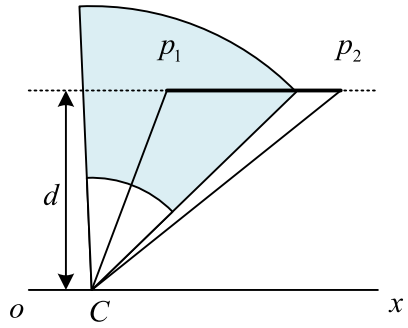


**FIGURE 9.** Coverage of a line segment by a camera.

The orientation and the FOV of the camera are $\alpha$ and $\theta$, respectively. If the detection boundary, i.e. the line with orientation of $\alpha - \theta/2$ or $\alpha + \theta/2$, directs towards $p_1$ or $p_2$, the covered line segment by the camera reaches maximum.

*Proof:* We use $\alpha_{\min}$ and $\alpha_{\max}$ to denote $(\arcsin(d/R_{\min} + \theta/2))$ and $(\pi\text{-}\arcsin(d/R_{\min} - \theta/2))$, respectively. The position of camera is denoted as $C$. If the angles $\langle \overrightarrow{p_1C}, \overrightarrow{ox} \rangle$ and $\langle \overrightarrow{p_2C}, \overrightarrow{ox} \rangle$ are in range $[\alpha_{\min}, \alpha_{\max}]$, and the detection boundary with the orientation of $\alpha - \theta/2$ or $\alpha + \theta/2$ directs towards $p_1$ or $p_2$, $\alpha = \alpha_{\min}$ or $\alpha = \alpha_{\max}$. Thus the covered part achieves maximum according to the ***Lemma* 1**. If $\langle \overrightarrow{p_1C}, \overrightarrow{ox} \rangle \in [\alpha_{\min}, \alpha_{\max}]$ and $\langle \overrightarrow{p_2C}, \overrightarrow{ox} \rangle \notin [\alpha_{\min}, \alpha_{\max}]$, the covered parts will also achieve the maximum when the detection boundary with the orientation $\alpha + \theta/2$ directs to $p_1$. In the Similar case with $\langle \overrightarrow{p_1C}, \overrightarrow{ox} \rangle \notin [\alpha_{\min}, \alpha_{\max}]$ and $\langle \overrightarrow{p_2C}, \overrightarrow{ox} \rangle \in [\alpha_{\min}, \alpha_{\max}]$, the corollary also holds true. If $\langle \overrightarrow{p_1C}, \overrightarrow{ox} \rangle$ and $\langle \overrightarrow{p_2C}, \overrightarrow{ox} \rangle \notin [\alpha_{\min}, \alpha_{\max}]$, the camera cannot cover any part of the line segment no matter where the orientation is.

According to ***Corollary* 2**, for a certain camera, we can adjust its orientation towards the end point of the line segment for maximizing the coverage. Therefore, we have obtained both the locations and the orientations of cameras that will bring the increase of coverage for the barriers.

Our proposed coverage enhancing method is summarized in ***Algorithm 1***.

### D. COMPLEXITY ANALYASIS

According to the ***Algorithm 1***, the computational complexity of uncovered segments detection is $O(mn)$, where $m$ is the number of the barrier lines and $n$ is the amount of the camera sensors. For each uncovered segment, the complexity of additional sensor selection for covering the gaps is $O(n)$. Therefore, the total computational complexity of Our proposed coverage enhancing method is $O(mn^2)$.

## V. PERFORMANCE EVALUATION

### A. NUMERICAL SIMULATION

In this section, we conduct some numerical simulations to evaluate the performance of our proposed method. The ROI is of size 400 * 1000. We firstly randomly deploy three camera groups alone the long boundary of the ROI with different focus lengths. Each kind of cameras group has the same number of cameras, and the max and min sensing ranges of the three camera groups are (200, 100), (300, 150) and (450, 250), respectively. The initial orientations of cameras are randomly distributed from 0 to $\pi$.

We firstly testify the effectiveness of our proposed method for improving the coverage. In this paper, we generally refer

**Algorithm 1** Coverage Enhancing Algorithm

```
Input: A rectangular ROI with w × h, and the positions and orientations of
    cameras which are randomly deployed on one boundary of the ROI.
The coverage of ROI is mapped into the problem of coverage of a group of barrier lines.
For i = 1 to m, m is the number of the barrier lines
    Find the uncovered segments on i^th barrier line.
    For j = 1 to n, m is the number of the gaps on the i^th barrier line
        Determine the optimal positions of the additional camera according to Corollary 1, and randomly select one position.
        Optimize the orientation of the camera according to Corollary 2.
        While (the j^th uncovered segment is not fully covered)
        {
            Find the uncovered gap on the j^th segment;
            Repeat (9) to (11)
        }
    End for
End for
```

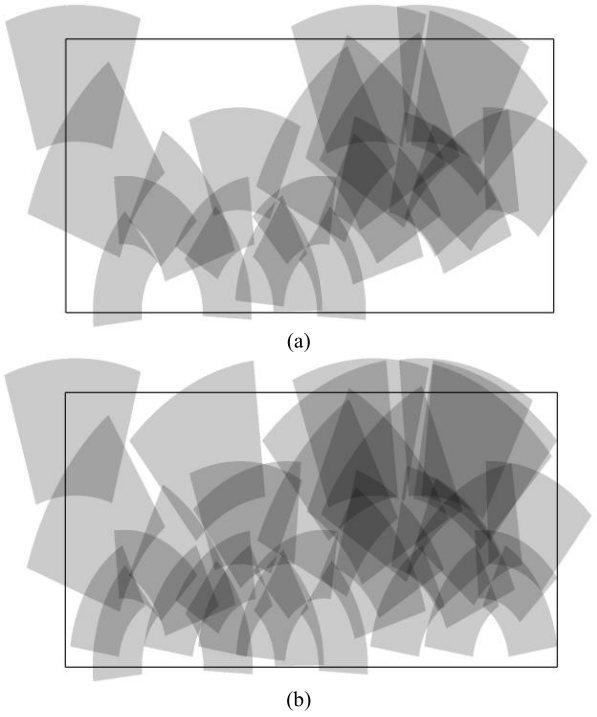


**FIGURE 10.** The effectiveness of proposed method in improving coverage.

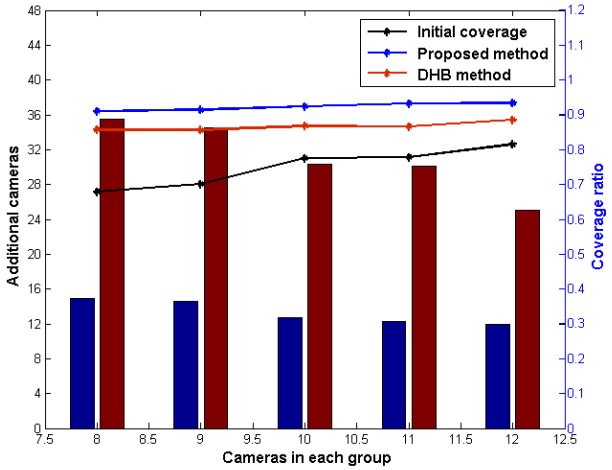


**FIGURE 11.** Coverage improvement and required additional cameras with different camera numbers.

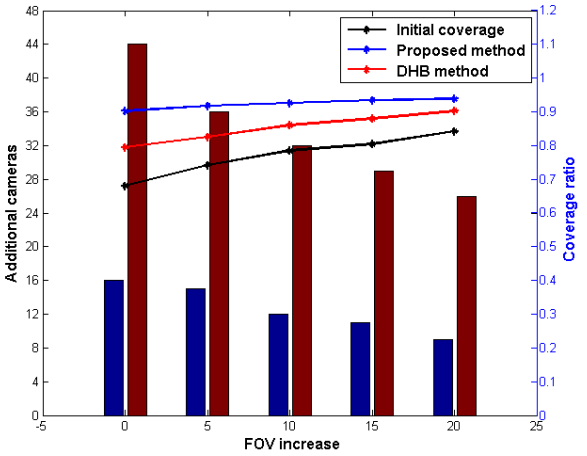


**FIGURE 12.** Coverage improvement and required additional cameras with different FOVs.

to the coverage performance of ROI as the ratio of the areas that have been covered successfully by camera networks to the entire area of ROI. Fig.10 (a) shows the result of ROI coverage by the initial deployed cameras. It is obvious that there is plenty of uncovered area in the ROI, and the coverage ratio by the cameras is 78.35%. Fig.10 (b) provides the ROI coverage by deploying additional cameras. The coverage ratio has been improved to 94.45% by 10 more cameras. Nevertheless, it is common sense that the increase of cameras will certainly enhance the sensing coverage. Thus, we analyze the comparisons of coverage improvement between our proposed method and other related methods in following sections.

In fact, the number of cameras and the FOVs of cameras would affect the coverage of ROI probability. Therefore, we investigate effects of the amounts and the FOVs of cameras on coverage performance. We set the number of cameras of each camera group from 8 to 12 with 1 camera increase in each round simulation. In order to evaluate the improvement of coverage, we take the direct heading-based method (we call it DHB method in this paper) [7] as a reference to evaluate the performance of our proposed method, which has been regarded as one of effective methods in covering a ROI with boundary deployment. In DHB method, the cameras directly head to the uncovered region, i.e. the orientations of cameras are perpendicular to the barrier line. Since the cameras are randomly deployed along the boundary side of ROI, we run 10 rounds of simulations for each sensor amount. The average value of the 10 round simulations is set as the final result in the performance evaluation.

The results of the coverage improvement by deploying additional cameras according to our proposed method and the DHB method are shown in Fig.11. The three lines show the coverage ratio of ROI with initial camera deployment, additional cameras deployment by proposed method and by DHB method, respectively. The blue bar and the red bar indicate the numbers of deploying additional cameras by our proposed method and the DHB method, respectively. It is obviously from that our proposed method has better performance in enhancing the coverage for the ROI compared with the DHB method, although both methods can improve the coverage. For example, the coverage of ROI is 77.5% with 10 randomly boundary deployed cameras in each group. In our proposed method, the coverage increases to 92.4% by deploying 12.7 additional cameras. DHB method increases to 86.2% by deploy 30.3 additional cameras. Besides, no matter how many cameras are initially deployed, the coverage of ROI will achieve more than 90% with 11 to 12 additional cameras in our method. The DHB method needs more than 25 additional cameras to achieve 80% coverage. It is also worthy noted that with the increase of the initial deployed cameras, the coverage of ROI grows in three cases, which is accordance with the fact that the numbers of cameras affect the coverage. The additional cameras become slightly less in our proposed method and the number in DHB method reduces sharper than our proposed method. The reason behind this is possibly that with the little increase of initial cameras, the barrier gaps cannot decrease significantly. Our proposed method is more effectively to heal the barrier gaps, and the DHB method uses more cameras to cover relatively few barrier gaps. Therefore, from this perspective, our proposed method is a kind of resource-saving methods compared with the DHB method.

In another scenario, we vary the FOVs of the three camera groups. The FOVs of cameras in the group 1 and the group 2 varies from 30° to 50° with 5° as the step size, and in the group 3, we let the FOVs of cameras change from 20° to 40° with 5° increase. Each group has 10 cameras that are randomly deployed at the boundary side of ROI. Fig.12 shows the comparison of the coverage improvement with FOV increase between the proposed method and the DHB method.

We can easily observe that with the increase of the FOVs, the coverage quality of ROI has also been improved, as shown

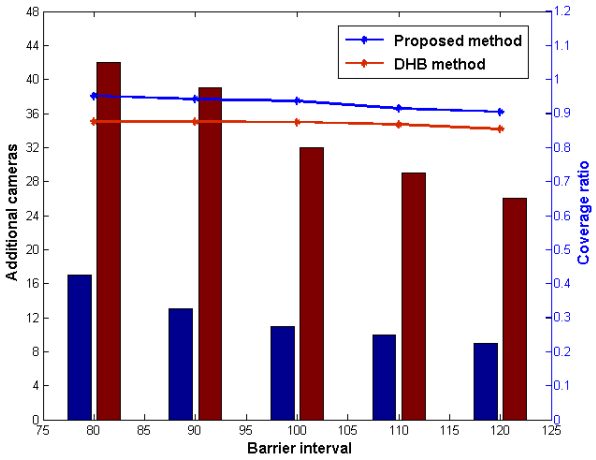


**FIGURE 13.** Coverage improvement and required additional cameras with different barrier intervals.

the three lines in Fig.12. It is because that the sensing area of each camera enlarges with the increase of the FOVs, and the coverage of ROI correspondingly become increasing. Note that the coverage improvement in the proposed method is superior to that in the DHB method. For example, the coverage of ROI by our proposed method is over 90% in each scenario with different FOVs. In DHB method, the coverage is less than 90% in every scenario. Besides, with the increase of the FOVs, although the required additional cameras become decreasing in both methods, our proposed method requires less additional cameras than the DHB method. In our proposed method, the required additional cameras are less than 15 in each scenario with different FOVs. In contrast, the DHB method needs more than 25 additional cameras.

We also conduct some experiments to illustrate the influence of barrier line intervals on the coverage performance. We set the barrier intervals from 80 to 120 with 10 as step size. Fig.13 shows the results of coverage performance and required additional cameras. We can observe that with the increase of barrier intervals, the coverage ratio of the ROI and the required additional cameras become decreasing in both methods. It is interesting that in our proposed method, when barrier interval is less than 100, the coverage of ROI changes little, but the required additional cameras reduce dramatically. When the barrier interval is larger than 100, the required additional cameras change little, but the coverage performance deteriorates relatively more. Thus, the interval selection method that the barrier interval is determined by the difference between $R_{max}$ and $R_{min}$ of the cameras with the small sensing ranges can be used as a compromise method between the coverage performance and cameras usage.

### B. SIMULATION FOR AIRPORT

In order to evaluate effectiveness of our proposed method in the actual airport surface surveillance, we use Guiyang airport in China as a case study. The Fig.14 (a) shows the digital map of Guiyang airport from Google map [26]. We use

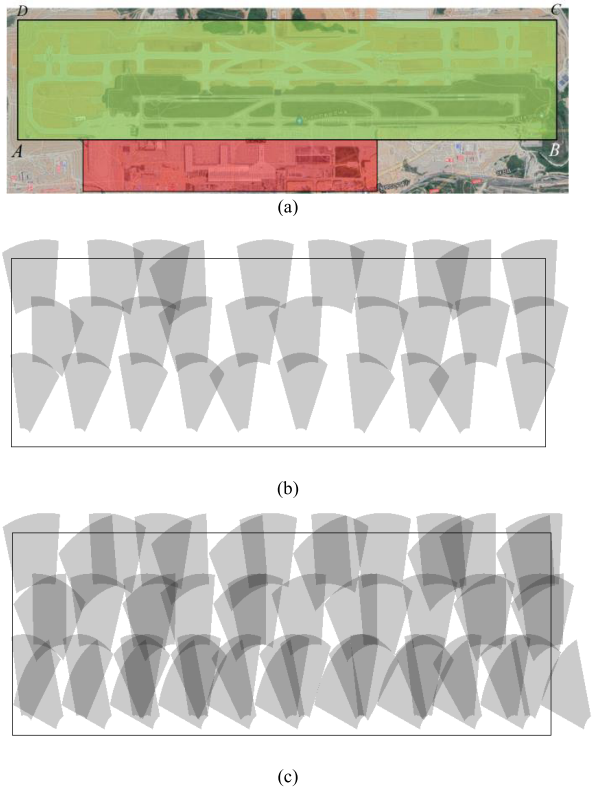


**FIGURE 14.** The simulation results in actual airport surface surveillance.

a rectangle *ABCD* to indicate the target ROI which contains all the taxiways, runways, aprons and other airside facilities, shown as the green region. The red region denotes the terminals and buildings on the land-side of the airport, and the cameras are usually installed on land-side facilities. Thus, in our study, we deploy 3 groups of cameras with different focus lengths alone the *AB* boundary. The size of the rectangle *ABCD* is $4.8km * 1km$. In each group of cameras, the settlement interval between any two cameras is $500m$, and the orientations of cameras are towards the air side. The max and min sensing ranges of the 3 camera groups are $(100m, 500m)$, $(450m, 800m)$ and $(750m, 1100m)$, respectively. Thus, in such deployment, the coverage of the airport surface is 64.8%, as shown in Fig.14 (b). According to our coverage enhancing method, by deploying 28 additional cameras, the coverage increases to 86.0%, as shown in Fig.14 (c). On contrast, we need 34 additional cameras to achieve the similar coverage by using the DHB method.

## VI. CONCLUSION

In this paper, we develop a coverage enhancing method in the airport surface surveillance. In order to address the problem of boundary deployed cameras, we map the area coverage problem into a barrier problem for a group of barrier lines. We analyze the relations between barriers and sensing models of cameras and find out the optimal locations and orientations of cameras to achieve maximum coverage. Based on the analysis, our proposed method contains detecting uncovered

barrier gaps and determining the optimal locations and orientations of cameras. The simulations show that our method could effectively improve the coverage in boundary deployed camera networks. Compared with similar coverage enhancing method, our algorithm uses less additional cameras to achieve more coverage. Therefore, our proposed method can be served as a useful tool for enhancing the coverage of camera network in airport surface surveillance.

## REFERENCES

[1] S. Vaddi, H.-L. Lu, and M. Hayashi, "Computer vision based surveillance concept for airport ramp operations," in *Proc. IEEE/AIAA 32nd Digit. Avionics Syst. Conf. (DASC)*, East Syracuse, NY, USA, Oct. 2013, pp. 1–35, doi: 10.1109/DASC.2013.6719648.
[2] F. Sbrizzi, S. Grazioso, M. Selvaggio, G. Di Maio, and G. Notomista, "Enhancing airplane boarding procedure using vision based passenger classification," in *Proc. IEEE 19th Int. Conf. Intell. Transp. Syst. (ITSC)*, Rio de Janeiro, Brazil, Nov. 2016, pp. 772–777.
[3] H.-L. Lu, J. Kwan, A. Fong, and V. Cheng, "Field testing of vision-based surveillance system for ramp area operations," in *Proc. AIAA Aviation Technol., Integr. Oper. Conf.*, Atlanta, GA, USA, vol. 2019, p. 3981.
[4] W. Wang, H. Dai, C. Dong, X. Cheng, X. Wangm, P. Yang, G. Chen, and W. Dou, "Placement of unmanned aerial vehicles for directional coverage in 3D space," *IEEE/ACM Trans. Netw.*, vol. 28, no. 2, pp. 888–901, Apr. 2020.
[5] J. Yu, S. Wan, X. Cheng, and D. Yu, "Coverage contribution area based $K$-coverage for wireless sensor networks," *IEEE Trans. Veh. Technol.*, vol. 66, no. 9, pp. 8510–8523, Sep. 2017.
[6] R. Elhabyan, W. Shi, and M. St-Hilaire, "Coverage protocols for wireless sensor networks: Review and future directions," *J. Commun. Netw.*, vol. 21, no. 1, pp. 45–60, Feb. 2019.
[7] B. Khalifa, A. M. Khedr, and Z. A. Aghbari, "A coverage maintenance algorithm for mobile WSNs with adjustable sensing range," *IEEE Sensors J.*, vol. 20, no. 3, pp. 1582–1591, Feb. 2020.
[8] Z. Liu and Z. Ouyang, "$K$-coverage estimation problem in heterogeneous camera sensor networks with boundary deployment," *IEEE Access*, vol. 6, pp. 2825–2833, 2017, doi: 10.1109/ACCESS.2017.2785393.
[9] X. Wang, Z. Tian, W. Wang, F. He, L. Zhao, and P. Gao, "A novel algorithm for barrier coverage based on hybrid wireless sensor nodes," *IEEE Access*, vol. 7, pp. 118866–118875, 2019, doi: 10.1109/ACCESS.2019.2936640.
[10] W. Li and Y. Wu, "Tree-based coverage hole detection and healing method in wireless sensor networks," *Comput. Netw.*, vol. 103, pp. 33–43, Jul. 2016.
[11] B. Wang, J. Zhu, L. T. Yang, and Y. Mo, "Sensor density for confident information coverage in randomly deployed sensor networks," *IEEE Trans. Wireless Commun.*, vol. 15, no. 5, pp. 3238–3250, May 2016.
[12] S. He, D.-H. Shin, J. Zhang, J. Chen, and Y. Sun, "Full-view area coverage in camera sensor networks: Dimension reduction and near-optimal solutions," *IEEE Trans. Veh. Technol.*, vol. 65, no. 9, pp. 7448–7461, Sep. 2016.
[13] K. A. Eldrandaly, M. Abdel-Basset, and L. Abdel-Fatah, "PTZ-surveillance coverage based on artificial intelligence for smart cities," *Int. J. Inf. Manage.*, vol. 49, pp. 520–532, Dec. 2019.
[14] T.-W. Sung and C.-S. Yang, "Voronoi-based coverage improvement approach for wireless directional sensor networks," *J. Netw. Comput. Appl.*, vol. 39, pp. 202–213, Mar. 2014.
[15] J. Jia, C. Dong, Y. Hong, L. Guo, and Y. Yu, "Maximizing full-view target coverage in camera sensor networks," *Ad Hoc Netw.*, vol. 94, Nov. 2019, Art. no. 101973.
[16] L. Zhang, T.-T. Liu, F.-Q. Wen, L. Hu, C. Hei, and K. Wang, "Differential evolution based regional coverage-enhancing algorithm for directional 3D wireless sensor networks," *IEEE Access*, vol. 7, pp. 93690–93700, 2019, doi: 10.1109/ACCESS.2019.2927805.
[17] X. Yang, Y. Wen, D. Yuan, M. Zhang, H. Zhao, and Y. Meng, "Coverage degree-coverage model in wireless visual sensor networks," *IEEE Wireless Commun. Lett.*, vol. 8, no. 3, pp. 817–820, Jun. 2019.
[18] Z. Han, S. Li, C. Cui, H. Song, Y. Kong, and F. Qin, "Camera planning for area surveillance: A new method for coverage inference and optimization using location-based service data," *Comput., Environ. Urban Syst.*, vol. 78, Nov. 2019, Art. no. 101396.
[19] E. Yildiz, K. Akkaya, E. Sisikoglu, and M. Y. Sir, "Optimal camera placement for providing angular coverage in wireless video sensor networks," *IEEE Trans. Comput.*, vol. 63, no. 7, pp. 1812–1825, Jul. 2014.
[20] P. Xu, I.-H. Chang, C.-Y. Chang, B. Dande, and C.-Y. Hsiao, "A distributed barrier coverage mechanism for supporting full view in wireless visual sensor networks," *IEEE Access*, vol. 7, pp. 156895–156906, 2019, doi: 10.1109/ACCESS.2019.2947262.
[21] C.-F. Cheng and C.-W. Wang, "The barrier-breach problem of barrier coverage in wireless sensor networks," *IEEE Commun. Lett.*, vol. 21, no. 10, pp. 2262–2265, Oct. 2017.
[22] J. Chen, B. Wang, W. Liu, L. T. Yang, and X. Deng, "Rotating directional sensors to mend barrier gaps in a line-based deployed directional sensor network," *IEEE Syst. J.*, vol. 11, no. 2, pp. 1027–1038, Jun. 2017.
[23] C.-F. Cheng and K.-T. Tsai, "Encircled belt-barrier coverage in wireless visual sensor networks," *Pervasive Mobile Comput.*, vol. 38, pp. 233–256, Jul. 2017.
[24] M. Khanjary, M. Sabaei, and M. R. Meybodi, "Barrier coverage in adjustable-orientation directional sensor networks: A learning automata approach," *Comput. Elect. Eng.*, vol. 72, pp. 859–876, Nov. 2018.
[25] Y. Wu and M. Cardei, "Distributed algorithms for barrier coverage via sensor rotation in wireless sensor networks," *J. Combinat. Optim.*, vol. 36, no. 1, pp. 230–251, Jul. 2018.
[26] *Google Map*. Accessed: Sep. 27, 2021. [Online]. Available: https://www.google.com/maps/@26.5428349,106.7989506,4987a,35y,270h/data=!3m1!1e3

**WEI LI** received the B.S. and Ph.D. degrees from the School of Mechatronical Engineering, Beijing Institute Technology, China, in 2003 and 2008, respectively. He joined the University of Electronic Science and Technology of China, in 2008. From 2010 to 2011, he was a Postdoctoral Member at the Center of Industrial Electronics, Polytechnic University of Madrid, Spain. In 2011, he became an Associate Professor with the University of Electronic Science and Technology of China. Currently, he is an Associate Professor with the School of Astronautics and Astronautics, Sichuan University, China. His research interests include quality of service of wireless sensor networks, object detection and identification in camera networks, and surveillance in camera networks.

**XIANGTONG WANG** received the B.S. degree from the School of Computer Science, Sichuan Normal University, in 2018, and the master's degree from the School of Aeronautics and Astronautics, Sichuan University, in 2021, where he is currently pursuing the Ph.D. degree with the School of Aeronautics and Astronautics. His research interests include computer vision and aircraft visual navigation and surveillance in camera networks.

**SONGCHEN HAN** received the B.S. degree in flying vehicle control from Harbin Engineering University, in 1987, and the M.S. degree in general dynamics and the Ph.D. degree in flying vehicle design from Harbin Institute of Technology, in 1990 and 1997, respectively. In 1990, he joined the School of Astronautics, Harbin Institute of Technology. From 2000 to 2014, he was a Professor with Nanjing University of Aeronautics and Astronautics. He is currently a Professor with the School of Aeronautics and Astronautics, Sichuan University. His research interests include air traffic control, surveillance in airport surface, and sensor networks.